Grid Generation Issues in the CFD Modelling of Two-Phase Flow in a Pipe

V. Hernandez-Perez, M. Abdulkadir and B.J. Azzopardi

Grid Generation Issues in the CFD Modelling of Two-Phase Flow in a Pipe

V. Hernandez-Perez*, M. Abdulkadir and B.J. Azzopardi
Process and Environmental Engineering Research Division, Faculty of
Engineering, University of Nottingham, University Park, Nottingham, NG7 2RD,
United Kingdom

Abstract
The grid generation issues found in the 3D simulation of two-phase flow in a pipe using
Computational Fluid Dynamics (CFD) are discussed in this paper. Special attention is
given to the effect of the element type and structure of the mesh. The simulations were
carried out using the commercial software package STAR-CCM+, which is designed
for numerical simulation of continuum mechanics problems. The model consisted of a
cylindrical vertical pipe. Different mesh structures were employed in the computational
domain. The condition of two-phase flow was simulated with the Volume of Fluid
(VOF) model, taking into consideration turbulence effects using the k-e model. The
results showed that there is a strong dependency of the flow behaviour on the mesh
employed. The best result was obtained with the grid known as butterfly grid, while the
cylindrical mesh produced misleading results. The simulation was validated against
experimental results.

NOMENCLATURE
In this section a list of symbols not defined in the main text is given

g	Gravitational acceleration [m/s^2]
k	Kinetic energy of turbulence [m^2/s^2]
n	number of phases [–]
t	Time [s]
u	Velocity [m/s]
μ	Dynamic viscosity [$kg/m.s$]
ρ	Material density [kg/m^3]
σ	Surface tension [N/m]
i, j	Space directions
q	Phase index

1. INTRODUCTION
The results obtained from a CFD simulation can be influenced by several parameters, of which not
least important is the mesh employed. A very simple but frequently encountered geometry in CFD
is a cylindrical pipe. In this geometry, however, a large variety of fluid flow phenomena can occur,
in some of them the physics involved can be very complex, such as in the case of multiphase flow.
Although the CFD simulation of two-phase flow in a pipe has been the subject of many works
reported in the literature, for instance Refs. [1–6], the literature review reveals that there is a lack
of detailed explanation of the mesh generation stage. Many of these works have been carried out in
a 2D domain, such as [1–3]. In practice, the CFD code documentation is often the best reference
tool available in the construction of the model.

There are different grid structures that can be applied in cylindrical pipe geometry. A natural
choice is a cylindrical polar grid, also called O-grid. Indeed some CFD packages provide readily
available tools to generate a cylindrical grid, for instance STAR-CD [7]. Simulations reported in

the literature using this grid topology in different phenomena include those of Erdal et al. [8], van Baten and Krishna [9] and Jeong et al. [10]. Other grid structures have also been employed in other works, for instance Cook and Behnia [5] used a rectangular Cartesian grid in a cylinder for the simulation of the motion of large bubbles, and they obtained good agreement between the simulation and experimental results. More recently [6] have used a butterfly-grid, for the simulation of continuous slug flow, which similarly produced good results.

However, the strengths and/or weaknesses of each mesh have not been well established, as no comparisons of such grids have been reported. Different mesh types have advantages and disadvantages related to cost, efficiency for flow solutions and automation of mesh-generation as stated in [11]. As a result, a CFD modeler, with no particular experience might have to face different challenges during the construction of the model. This subject has been central to personal communications with colleagues. After a critical literature review, we became aware of the absence of a suitable study about this matter, so we decided to clarify this issue.

This work aims to make a contribution to the CFD community regarding the effect the mesh used in the computational domain may have on the results of the simulation.

2. NUMERICAL MODEL

It is difficult to cover in one single paper all aspects of the pitfalls that can be found when selecting a particular mesh for a CFD simulation. In this work we discuss briefly some points that are relevant to the case of the simulation of flow structures and their interaction in gas-liquid flow in a vertical pipe.

2.1. Computational domain

In order to carry out this study, an individual cylindrical volume was created as one entity, using the tools available in the software STAR-CD, see Figure 1. A full 3-dimensional domain was considered, as the flow simulated has been found not to be symmetrical from real experiments, such as those reported by Azzopardi et al. [12] and Hernandez-Perez et al. [13]. Employed Wire-Mesh Sensors (WMS) to look at the flow distribution and showed that the classical Taylor bubble shape is rarely observed when the pipe diameter is increased. In this work the pipe diameter is 67 mm as it is in Ref. [12] and Ref. [13], but a shorter pipe length was used, 1 m as opposed to 6 m in Ref. [12] and Ref. [13], as this length is enough to carry out a test on the performance of the mesh with relatively moderate computational effort.

Similar to the experimental work of Ref. [12] and Ref. [13], air and silicone oil flow is supplied at the inlet section of the computational flow domain (pipe), then the two-phase mixture flows along the pipe, and is finally discharged through the outlet at atmospheric pressure. The relevant liquid physical properties are density, viscosity and surface tension, whose values are 900 kg/m^3, 0.00525 kg/ms and 0.02 N/m, respectively.
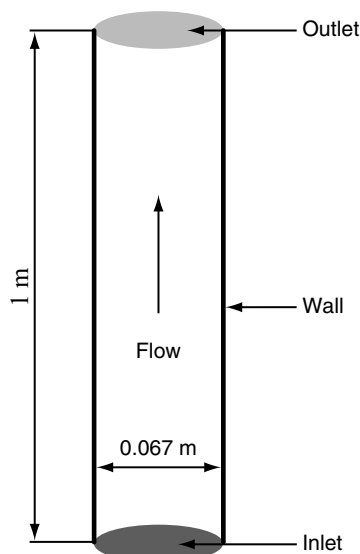

Figure 1. 3D Geometry of the computational domain

2.2. Grid generation

The mesh has a great influence on the solver convergence and solution of every CFD simulation, as it is important to keep high mesh quality standards to ensure convergence and the accuracy of the simulation. Four different mesh structures where developed in order to carry out the simulations for this work. In the first instance, the number of cells generated in all cases was 75000 (500 in the cross section and 150 in the length) meaning a similar spatial resolution to that of the WMS used in [12] and [13], which has a spatial resolution given by the number of crossing points (or measuring points) in a mesh of 24×24 wires in the cross sectional area of the pipe. Details of the WMS operation can be found in Da Silva et al. [14]. In terms of the time resolution, a time step of 0.0001 s has been employed. This overcomes the time resolution of all the measuring instruments used in [4]. This mesh density was selected based on the grid convergence study carried out in Hernandez-Perez [6], where a mesh with a 150000 cell in an inclined pipe geometry of 6 m length and 38 mm diameter was found to be adequate for an inlet flow condition that consists of liquid and gas superficial velocities of 0.7 m/s and 1.6 m/s, respectively. Moreover in the present work, lower velocities are used. A mesh refinement was carried out in some cases, as explained below, in order to verify that the result obtained was an effect of the structure of the mesh. The simulations were run in a 4-processor machine and the simulation running time was in the order of hundreds of hours (seconds of real time), which allows for the gas phase to travel from the bottom to the top of the pipe. However, this can be reduced by increasing the number of processors running in parallel. Furthermore, computer power is expected to increase in the years to come.

The first mesh employed consists of a polar cylindrical mesh (O-grid) as illustrated in Figure 2. In this type of grid there is one family of grid lines forming concentric circles around the centre of the cylinder and the other family of grid lines are radially directed. This was tested due to the fact that the software STAR-CD has the tools for creating this grid topology by specifying the number of cells in radial, circumferential and axial directions. For this topology, both complete and half geometry were tested, in an effort to overcome the pitfalls found with the full pipe geometry, as discussed in section 3.

The second mesh used is known as butterfly grid, Figure 3. In this mesh, a Cartesian mesh is used in the centre of the pipe combined with a cylindrical one around. It requires multiple blocks but generally has the best grid quality in terms of orthogonality and mesh density. The construction of this mesh requires a more elaborated procedure, but it can be automated by implementing a macro in the STAR-CD software.

A third mesh was created based on a rectangular structure, also called H-grid, which is formed by orthogonal grid lines. This can be employed to topologically adapt a single rectangular grid to a circular shape, as shown in Figure 4.

An unstructured mesh that fits the circular cross sectional area of the cylinder is the pave grid. Figure 5 shows this type of grid topology. In this case the cells are arranged in an arbitrary fashion
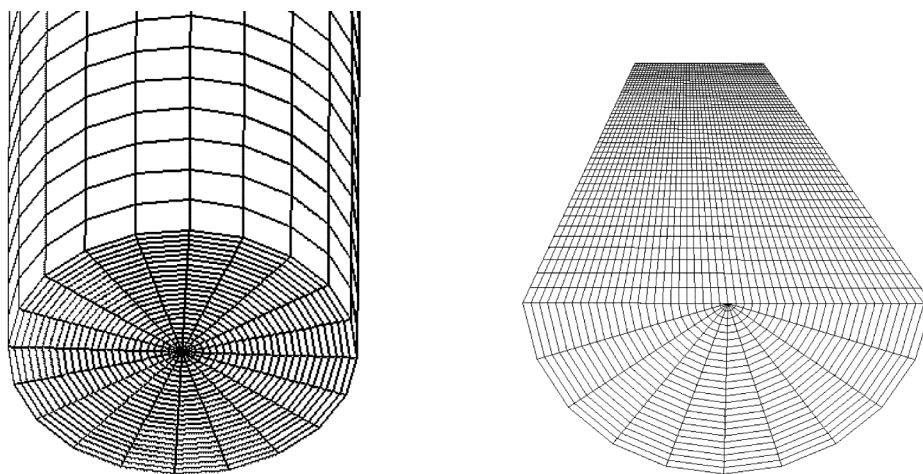

Figure 2. Polar cylindrical mesh (O-grid) in 3D vertical pipe, complete geometry (left) and half geometry (right)
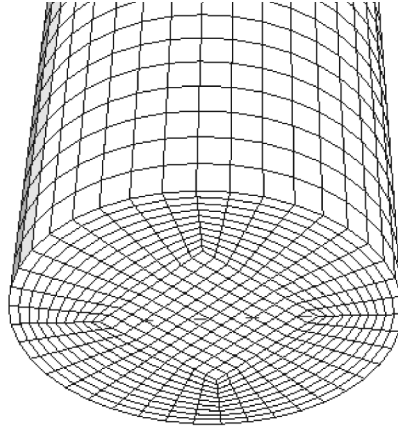
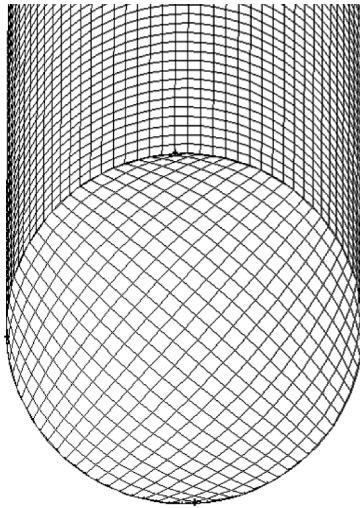Figure 3. Butterfly grid in 3D vertical pipe

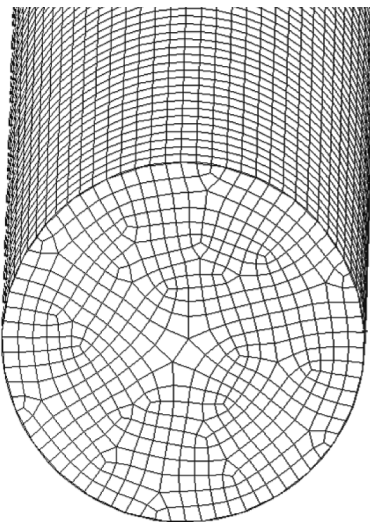Figure 4. Rectangular H-grid in 3D vertical pipe

Figure 5. Unstructured pave grid in 3D vertical pipe

to fill the cross section of the computational domain, the grid points are not connected with a regular topology and cannot be described with a function between the number of cell and the number of its neighbors. For this reason, a memory and CPU overhead is expected for this unstructured grid, which is a disadvantage. This mesh was imported from CFD software and read into STAR-CCM.

2.3. Governing equations

In the present work, isothermal motion of an incompressible two-phase slug flow has been considered as the flow scenario. This condition has been simulated with the Volume of Fluid (VOF) model, initially presented by Hirt and Nichols [15] based on Eulerian-Eulerian approach. In addition, STAR-CCM+ [7] uses a High Resolution Interface Capturing Scheme (HRIC) based on the Compressive Interface Capturing Scheme for Arbitrary Meshes (CISCAM) introduced by Ubbink [16] and enhanced by Peric and Muzaferija [17]. In the VOF method, the fields for all variables and properties are shared by the phases and represent volume-averaged values, as long as the volume fraction of each of the phases is known at each location. Therefore a single set of equations is solved through the flow domain, which are dependent on the volume fractions of all phases through the properties ρ and μ. For a two-phase system, ρ and μ are linked to the volume fraction through the following relations: $\rho = \alpha\rho_1 + (1\text{-}\alpha)\rho_2$, $\mu = \alpha\,\mu_1 + (1\text{-}\alpha)\mu_2$. The continuity equation, equation (1), ensures a mass balance in the flow domain. The momentum equation, equation (2), accounts for the forces acting on the system. Once the Reynolds averaging approach for turbulence modelling is applied, the Navier-Stoke equations can be written in Cartesian tensor form as:

$$\frac{\partial\rho}{\partial t} + \frac{\partial(\rho u_j)}{\partial x_j} = 0 \tag{1}$$

$$\frac{\partial}{\partial t}(\rho u_i) + \frac{\partial}{\partial x_j}(\rho u_i u_j) = \frac{\partial P}{\partial x_i} +$$
$$\frac{\partial}{\partial x_j}\left[\mu_{eff}\left(\frac{\partial u_i}{\partial x_j} + \frac{\partial u_j}{\partial x_i} - \frac{2}{3}\delta_{ij}\frac{\partial u_i}{\partial x_i}\right)\right] + \frac{\partial}{\partial x_j}\left(-\rho\overline{u'_i u'_j}\right)_i \tag{2}$$

where u_i is the i component of the fluid velocity u, x_j is the j spatial coordinate, P is the static pressure, μ_{eff} is the effective viscosity, δ_{ij} is the Kronecker delta and $-\rho\overline{u'_i u'_j}$ the Reynolds stresses

The tracking of the interface(s) between the phases is accomplished by the solution of a continuity equation for the volume fraction (α) of one (or more) of the phases. The volume fraction field will have values as follows: $\alpha = 0$ if the cell is empty, $\alpha = 1$ if the cell is full, $0 < \alpha < 1$ if the cell contains the interface between the two fluids. For the q_{th} phase, this equation has the following form:

$$\frac{\partial\alpha_q}{\partial t} + \frac{\partial\left(\alpha_q u_j\right)}{\partial x_j} = \frac{S\alpha_q}{\rho_q} \tag{3}$$

Where S is a source, the volume fraction equation will not be solved for the primary phase; the primary-phase volume fraction will be computed based on the condition:

$$\sum_{q=1}^{n}\alpha_q = 1 \tag{4}$$

The surface tension at an interface between two fluids is the result of an imbalance of the attraction forces between molecules at the interface between two fluids. In the VOF model, surface tension is introduced as a body force acting on grid cells that contain the interface by adding a momentum source term to the momentum equation. In STAR-CCM+ the surface tension model is the Continuum Surface Force (CSF) model proposed by Brackbill et al. [18]. The pressure drop across the surface depends upon the surface tension value.

It is important to keep in mind that the VOF method has its limitations. The fact that the two fluids are assumed to share the same momentum equations restricts the suitability of the VOF method for cases where the difference in the velocity between the two fluids is significant.

The solution to the set of equations has been obtained using the software package STAR-CCM+. For the calculation of fluxes at control volume faces required by the VOF model, a second order discretization scheme was used, as recommended by the code documentation. In addition, a value of 1 was assign to the sharpening factor, as surface tension effects are taken into account in the simulation. The sharpening factor gives a better resolution of the interface.

It is important to take into consideration the turbulence in the numerical simulation since it is evident that even in cases of low flow rates, the Taylor bubbles rising through the liquid create a developing film around themselves and a wake at the tail. A high velocity gradient is expected to occur at the gas-liquid interface, with the gas moving much faster than the liquid phase. In order to simulate turbulence, the standard k-ε model, Launder and Spalding [19], which requires that the flow is fully turbulent, was used for several reasons; the model is computationally-efficient, is implemented in many commercial codes, the pipe geometry is not complicated and it has demonstrated capability to simulate properly many industrial processes, including multiphase flow. Shen et al. [20] applied k-ε model together with VOF. The model is described by the following elliptic equations required as closure for the Reynolds Average Navier Stokes (RANS) equations:

$$\rho u_j \frac{\partial k}{\partial x_j} = \frac{\partial}{\partial x_j}\left(\frac{\mu_t}{\sigma_k}\frac{\partial k}{\partial x_j}\right) + \mu_t \frac{\partial u_j}{\partial x_i}\left(\frac{\partial u_i}{\partial x_j} + \frac{\partial u_j}{\partial x_i}\right) - \rho\varepsilon \qquad (5)$$

$$\rho u_j \frac{\partial \varepsilon}{\partial x_j} = \frac{\partial}{\partial x_j}\left(\frac{\mu_t}{\sigma_\varepsilon}\frac{\partial \varepsilon}{\partial x_j}\right) + C_1\mu_t \frac{\varepsilon}{k}\frac{\partial u_j}{\partial x_i}\left(\frac{\partial u_i}{\partial x_j} + \frac{\partial u_j}{\partial x_i}\right) - C_2 \frac{\varepsilon}{k}\rho\varepsilon \qquad (6)$$

In the above equations, k is the turbulent kinetic energy; ε is the dissipation rate of k. σk, $\sigma\varepsilon$, C_1 and C_2 are constants whose values are 1.0, 1.3, 1.44 and 1.92 respectively, u_i is the i component of the fluid velocity u, x_j is the j spatial coordinate. The fluid viscosity must be corrected for turbulence in the Navier-Stokes equations employing an effective viscosity $\mu_{eff} = \mu + \mu_t$ where μ is the dynamic viscosity and μ_t is the turbulent viscosity.

2.4. Boundary and initial conditions

Once the mesh was generated, the boundaries of the computational domain are specified. Boundary type specifications define the physical and operational characteristics of the model at those topological entities that represent model boundaries.

At the wall the conditions were assumed to be no slip boundary, and the wall function approach is used. The no slip condition (v = 0) is the appropriate condition for the velocity component at solid walls, since Fluid in contact with the wall is stationary. At the inlet, velocities for both phases were prescribed as superficial velocities: liquid 0 m/s and gas 0.15 m/s. The phases were clearly defined with the primary phase as silicone oil and the secondary phase as air. The volume fraction and density of each phase were both prescribed at the inlet. The summary of the boundary specifications is as follows:

Inlet ………………Velocity inlet
Outlet ………Pressure outlet
Wall…………………Wall

The domain was initially represented as full of liquid phase with a velocity field equal to zero.

2.5. Solution algorithm

In order to numerically solve the system of governing partial differential equations, discretisation of the equations has been carried out using a Finite Volume Method (FVM) with an algebraic segregated solver and co-located grid arrangement, as implemented in STAR-CCM+ [7]. In this grid arrangement, pressure and velocity are both stored at cell centres. Details of the discretisation (FVM) can be found elsewhere (e.g. Versteeg and Malalasekera [21]) and are hence omitted here. Since STAR-CCM+ uses a segregated solver for VOF, the continuity and momentum equations

need to be linked. Various techniques are reported in the literature. However, the SIMPLE algorithm, which stands for Semi-Implicit Method for Pressure-Linked Equations, Patankar and Spalding [22], is applied to control the overall solution because of its good performance to find a fast converged solution. In addition, the iterative solver was speeded up tremendously by using an Algebraic Multigrid (AMG) technique to yield a better convergence rate.

All simulations in this work are performed under time dependent conditions, due to the unsteady nature of the problem. For the time dependent solution scheme, the main controlling factor is the time step. This is set in such a way that it gives a small number of time steps as possible whilst maintaining a smoothly converging solution. If a large time step is chosen, then big changes are produced in the solution and it is therefore likely to diverge. Within each time step, iterations are carried out to resolve the transport equations for that time interval. As long as the time step is small enough for the solution to convergence, the smaller the time step, the fewer iterations per time step are required. In addition, for this iterative process to converge, it may be necessary to control the change of the variables from a single iteration to the next. This is achieved by using under relaxation factors. Under relaxation factors of 0.3, 0.7 and 0.8 respectively were applied on pressure, momentum and turbulence kinetic energy parameters, as recommended by STAR-CCM+ [7].

An assessment of the degree to which the solution has converged can be obtained by plotting the residual errors for each equation at the end of each time step. For a well-converged simulation, the maximum residual obtained was set to be around 10^{-3}; it is possible that a residual increases after any particular time step, but it does not necessarily imply that the solution is diverging. It is usual for residuals to occasionally get larger, such as at the beginning of a run. In the present work it was observed that the residuals corresponding to the continuity and Turbulence Dissipation Rate are usually higher than the others.

3. RESULTS AND DISCUSSION
As described in section 2.1, the computational domain was initially filled with the liquid phase, and the gas phase is introduced from the bottom of the pipe. Figure 6 shows the results obtained for the velocity field in a section far away from the bottom, just after a few time steps, at the beginning of the simulation. Because at that moment the pipe is occupied by the liquid phase, this scenario is no different from that of single phase flow simulation and offers a simplified situation to investigate the effect of the grid. It can be observed that there is a difference in the way the velocity vectors are in the different meshes used. For the case of the cylindrical O-grid, the parabolic velocity profile is not clearly attained; instead, the velocity profile is almost flat, resembling turbulent flow. As shown in the results, a misleading behaviour of the flow is achieved when this mesh is used. After careful examination, it was detected that one of the reasons for this misbehaviour was that when this grid was generated in STAR-CD, wall-type boundaries are formed inside the computational domain, at 0 and 360º, and they overlap. This interferes with the actual motion of the flow. In order to avoid this problem, the "assemble" tool in STAR-CD was used. However this did not produce good simulation results either. In addition, and for comparison purposes, half of the computational domain was used with half the number of cells, in order to keep the mesh density constant. In this case, a symmetry type boundary was used, and the results obtained were better than those obtained with the whole cylinder but not satisfactorily good. Indeed the residuals for the turbulent dissipation rate do not fall below 1 unless a time step smaller than 1e5 is used. On the contrary, the velocity field obtained with the rectangular, butterfly and pave grids are as expected. Indeed, for the butterfly mesh, the expected parabolic velocity profile is obtained when the pipe is full of liquid. This suggests that the mesh employed can have an effect on the simulation for the case of single phase flow.

When the air is introduced from the bottom, an interaction between the gas and liquid phases in the pipe takes place and a two-phase mixture is formed. The interfaces between the phases can take different configurations called flow patterns. Figure 7 shows the results obtained for the phase distribution in a section that begins at the bottom of the pipe or flow domain. Although the gas phase flows at the centre of the pipe at the bottom, for the O-grid, it eventually moves to the side, randomly, as it moves upwards. This can be thought of as a consequence of the misbehavior of the velocity field shown in Figure 6, because the velocity field determines movement of the bubbles and the interaction amongst them. In addition, the flow pattern appears to be characterized by dispersed flow of small bubbles, as coalescence is difficult to achieve under these circumstances.
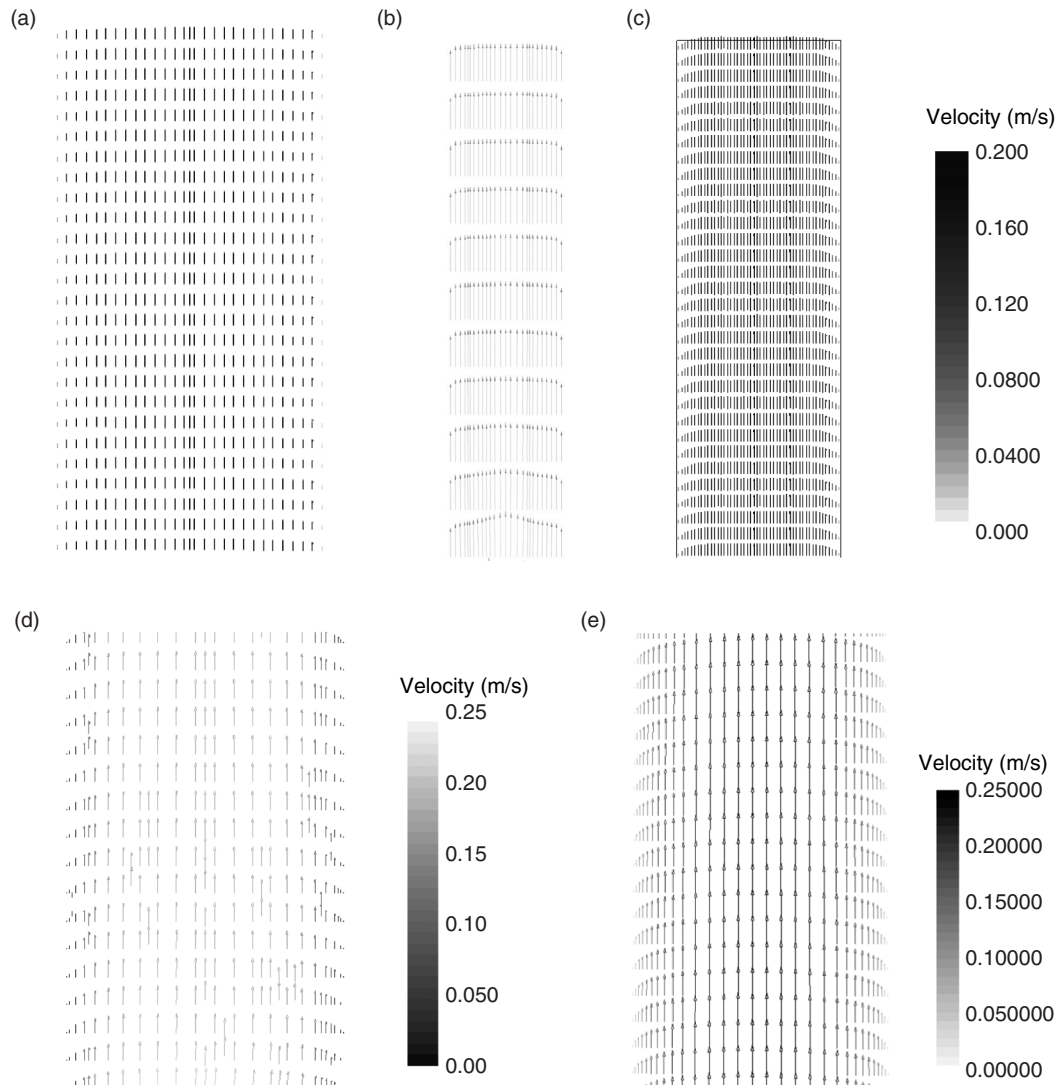
Figure 6. Velocity field with pipe full of liquid, superficial velocities: liquid 0 m/s and gas 0.15 m/s. a) complete cylindrical O-grid, b) half cylindrical O-grid, c) rectangular H-grid, d) pave grid, e) Butterfly grid

On the contrary, the contours of phase distribution obtained with the H-grid, pave grid and butterfly grid are very similar to those experimental results reported by Ref.[4], in terms of the phase distribution, as shown in Figure 7. These flow structures (liquid slugs and Taylor bubbles) are difficult to visualize using conventional visualization techniques.The phase distribution contours also seem to be associated with the velocity field shown in Figure 6, with the gas flowing at the centre of the pipe as bubbles of different sizes, driven by the velocity field. This is also in agreement with observations reported by Pinto and Campos [23] and Pinto et al. [24] in terms of the merging of small bubbles with the leading Taylor bubble at small separation distance.

One aspect that affects the behaviour of the flow structures in two-phase flow is the velocity field. Figure 8 presents the CFD-obtained velocity field for the different meshes employed in the present investigation. It shows the velocity field in the front of the leading Taylor bubble that is produced when air is supplied from the bottom of the pipe full of liquid. This is similar to the motion of a single Taylor bubble in a liquid, which has been simulated with CFD by other authors, and the behaviour of the velocity field is well known. However, most work has been directed to the motion of single Taylor bubble in vertical pipe where flow symmetry can be considered, as done
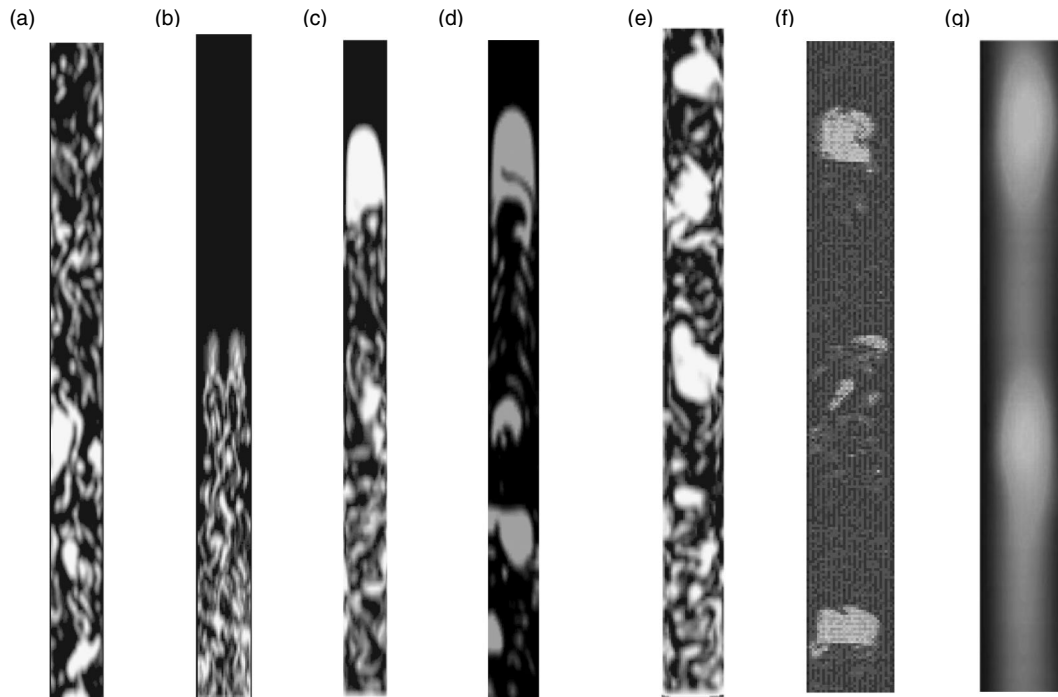
Figure 7. Contours of phase distribution, same inlet flow condition as in Fig. 4. The liquid and gas phases are represented by dark and light colours, respectively. a) complete cylindrical O-grid, b) half cylindrical O-grid, c) rectangular H-grid, d) pave grid, e) Butterfly grid. f) and g) are experimental results reported in [4], they were obtained using instruments known as Wire Mesh Sensor (WMS) and Electrical Capacitance Tomography (ECT), respectively

by Mao and Dukler [2]. Clarke and Issa [3] achieved the modelling of the motion of a periodic train of Taylor bubbles in vertical flow by imposing cyclic conditions at the inlet and outlet of the slug unit based on the assumption that the flow pattern repeats itself over consecutive slug units. They also assumed that the base of the bubble is flat. Similarly, Bugg et al. [4] developed a numerical model of Taylor bubbles rising through stagnant liquids in vertical tubes. Experimentally it is difficult to obtain measurements of the velocity field. Shemer et al. [25] used an experimental approach involving Particle Image Velocimetry (PIV) to measure the turbulent velocity field in vertical flow. By comparing the results obtained with the different grid topologies employed, it can be observed that, in particular, at the front of the Taylor bubble, the velocity field differs for the case of the O-grid.

As for the contours of phase distribution for both the Taylor bubble and the liquid slug body reported in Figure 9, the CFD simulation, results obtained with the butterfly-grid are in good agreement with the Wire Mesh Sensor (WMS) results. This agreement suggest that the CFD simulation can be considered to be useful for obtaining other flow parameters that characterize the internal structure of the flow that are difficult to measure experimentally, such as the velocity field, phase distribution and even the turbulence intensity [20].

In order to make the comparison with experimental data more quantitative, the translational rising velocity of the leading Taylor bubble has been calculated for the simulation as well as for the experimental work. Figure 10 shows the results the calculation process.

Time series of cross sectional void fraction have been obtained at two different locations along the pipe separated by a distance. The butterfly grid has been used. For the experiment, an Electrical Capacitance Tomography (ECT) sensor was employed. The ECT contains two measuring planes, as described by Abdulkareem et al. [4]. A cross correlation is carried out between the two signals in order to determine the time delay. Finally the velocity has been calculated by dividing separation
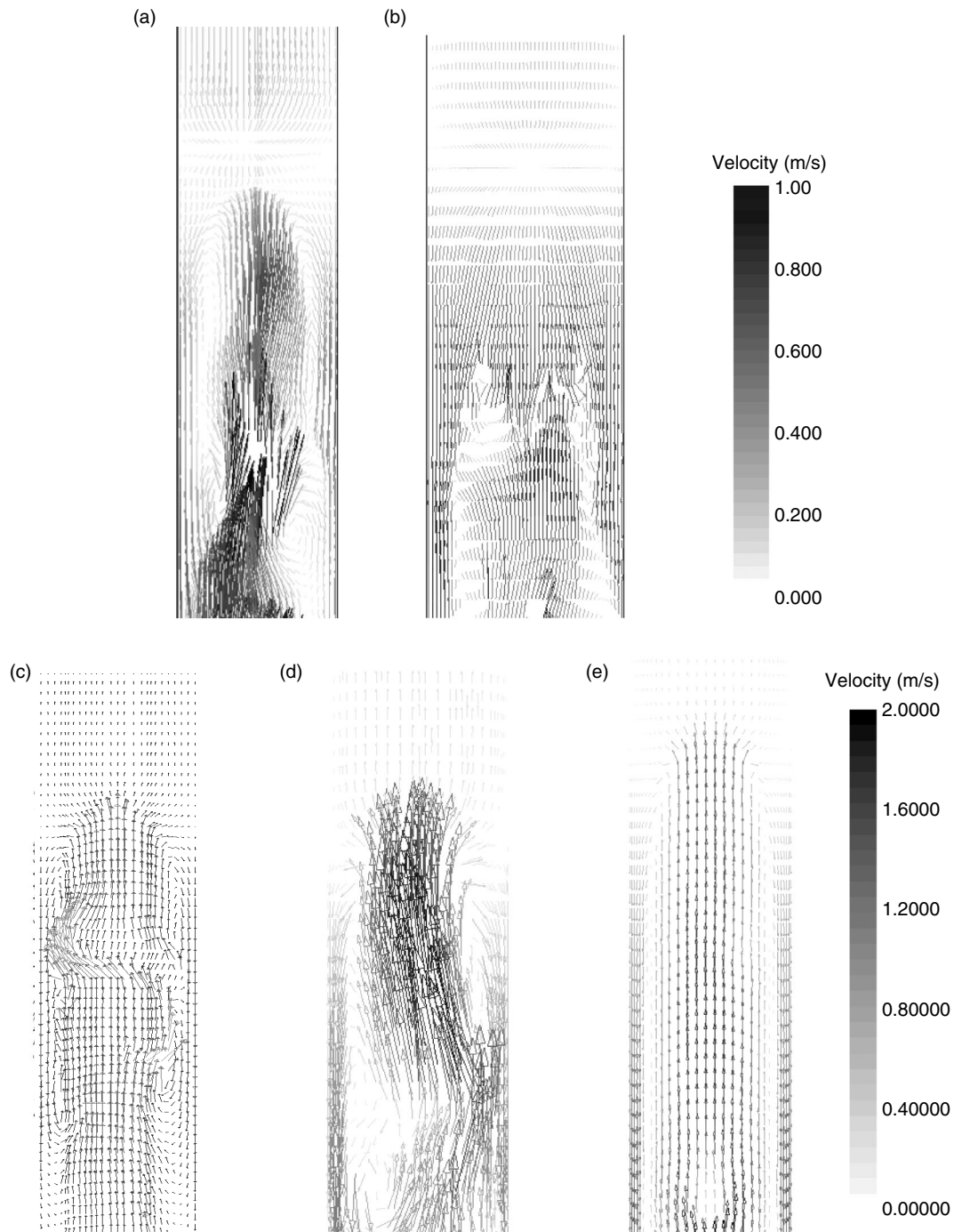
Figure 8. Velocity field at the front of the leading Taylor bubble, superficial velocities:
liquid 0 m/s and gas 0.15 m/s. a) complete cylindrical O-grid, b) half cylindrical O-grid,
c) rectangular H-grid, d) pave grid, e) Butterfly grid

distance by delay time. The values obtained are 0.506 m/ s for the simulation and 0.494 m/ s for the experiment, which shows good agreement.

As it happens, the mesh density can also have an effect on the performance of the mesh topology. Further simulations have been carried out using finer grids, particularly for the cases of the cylindrical, pave and rectangular grids. Here, the number of cells was increased to 150 000. It is worth mentioning that for a higher mesh density, a smaller time step is required. The results are presented in Figure 11. These show that no better results are achieved by increasing the mesh density.
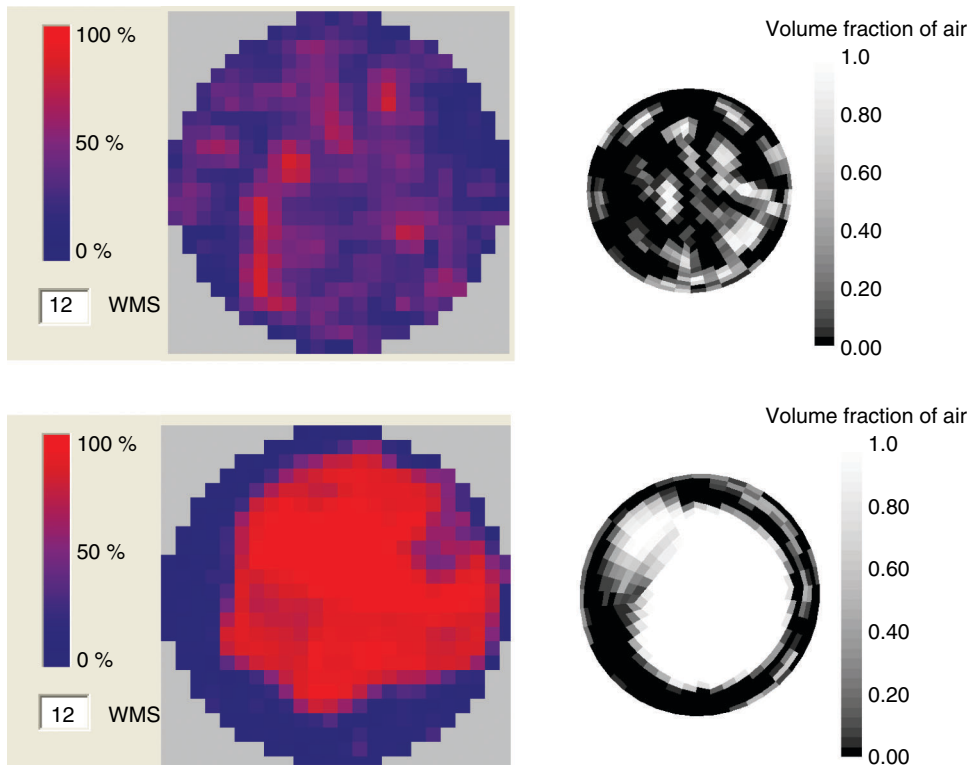
Figure 9. Comparison between contours of phase distribution in the cross sectional area (volume fraction of air). Screenshots taken at a liquid superficial velocity of 0 m/s and a gas superficial velocity of 0.15 m/s. Liquid slug body above; Taylor bubble below. In the left Wire Mesh Sensor and in the right CFD results
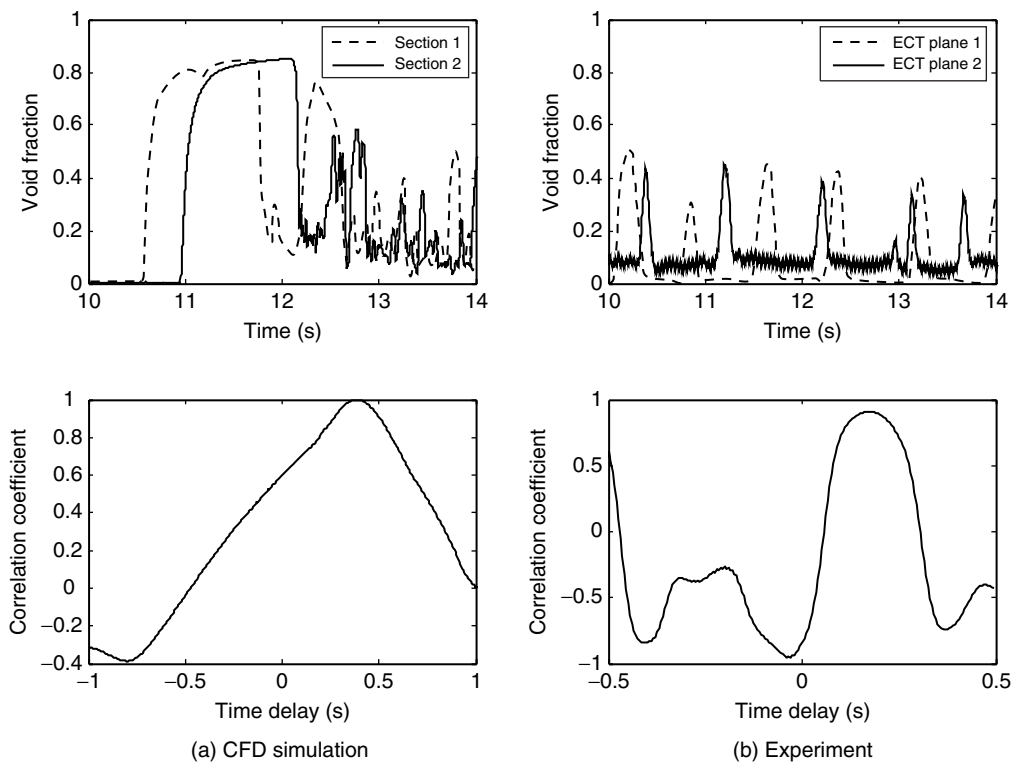

(a) CFD simulation

(b) Experiment

Figure 10. Time delay of a Taylor bubble passing through two different positions along the pipe, same inlet flow condition as in Figure 9
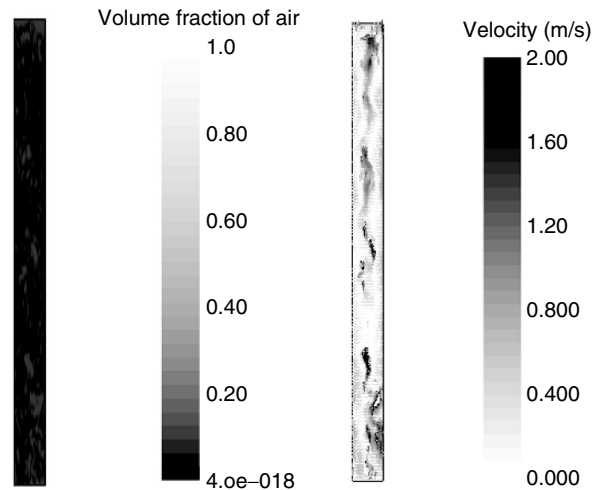
Figure 11. Contours of phase distribution on the left and velocity on the right, after mesh refinement, cylindrical o-grid, same inlet flow condition as in Figure 9
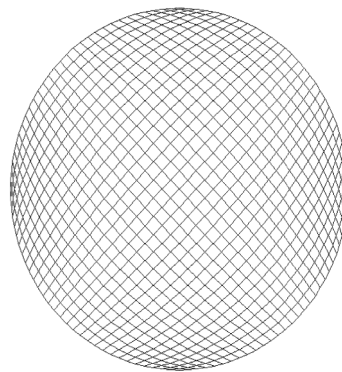

Figure 12. Rectangular grid after refinement

On the contrary, for the case of the rectangular H-grid, the quality of the mesh is reduced significantly, Figure 12, with the skewness values for the cells at the corners approaching 1 very rapidly as the mesh density increases. In the case of butterfly and pave grid a better resolution is obtained for the interface, however it is not worth the extra cost in terms of computing effort. In order to maintain a good aspect ratio, the mesh density in the axial direction needs to be increased accordingly.

The aforementioned results showed an underperformance of the O-grid. This can be explained by the fact that when a grid is created as a structured mesh in cylindrical coordinated system, an undesirable effect will happen for the cells near the centerline, which will have an acute angle. The narrowness of the cells would increase as the mesh is refined. This reduces the mesh quality in terms of skewness and orthogonality. This type of mesh, however, is very suitable for geometries such as an annulus and external flows. A high quality mesh increases the accuracy of the CFD solution and improves convergence relative to a poor quality mesh. The quality of the mesh is measured in terms of the skewness and aspect ratio. As part of the finite volume method, it is required that the points of the grid are arranged so that they can be grouped into a set of volumes and the governing equations can be solved by equating various flux terms through the faces of a fluid element in order for the fluxes to be balanced.

On the contrary, a butterfly grid is an ideal configuration to make use of the hexahedral mesh properties. Similar results were obtained with the H-mesh and pave mesh. However, the butterfly mesh has better aspect ratio cells with limited skewness. It allows for a good representation of the

boundary layer and it is adequately stretched along the longitudinal axis. The results obtained with the butterfly grid are in agreement with those obtained by Ref. [4]. Perhaps the major drawback of the butterfly grid is the time and expertise required for it to be built. In the present work we focus on the grid generation pitfalls. Detailed analysis of the flow behavior, in terms of several parameters, such as the void fraction profile and average void fraction, has been carried out elsewhere, e.g. Szalinski et al. [26]. The issues found in the mesh generation for the cylindrical geometry can be taken into consideration when more complicated geometries, but commonly employed, are modeled, such as T-junctions, branched bends, etc.

4. CONCLUSIONS

A comparison of different grid topologies used in the Computational Fluid Dynamics simulation of gas-liquid flow in a pipe has been carried out and the following conclusions can be drawn:

The polar O-grid with complete and half of the geometry did not succeed in producing a reliable simulation, regardless of the mesh density. The rectangular H-grid can produce reasonably good results at moderate grid density but it fails when the mesh is refined, as skewness is increased for cells at the corners. The pave grid and butterfly grid produced good results, as they are in agreement with those obtained using tomography techniques experimentally and reported by Ref. [4]. However, the best agreement was obtained with the butterfly grid. This grid allows refining the mesh closed to the wall and prevents a singularity at the centre of the pipe. The mesh at the centre could be coarse and at fine near the wall. The butterfly type of grid is therefore highly recommended for the simulation of two-phase flow in a pipe.

ACKNOWLEDGEMENTS

REFERENCES

[1]   Mao, Z. S. and Dukler, A. E., The motion of Taylor bubbles in vertical tubes. I. A numerical investigation for the shape and rise velocity of Taylor bubbles in stagnant and flowing liquid, Journal of computational physics, 1990, Vol. 91, pp. 132–160.

[2]   Clarke, A. and Issa, R. I., A numerical model of slug flow in vertical tubes, Computers & Fluids, 1997, Vol. 26, No. 4, pp. 395–415.

[3]   Bugg, J.D., Mack, K. and Rezkallah, K.S.. A numerical model of Taylor bubbles rising through stagnant liquid in vertical tubes. Int. J. Multiphase Flow, 1998, 24, pp. 271–281.

[4]   Abdulkareem, L.A., Hernandez-Perez, V., Azzopardi, B.J., Sharaf, S., Thiele, S. & Da Silva, M., Comparison of different tools to study gas-liquid flow. ExHFT-7, 28 June – 03 July 2009, Krakow, Poland.

[5]   Cook, M. and Behnia, M., Bubble motion during inclined intermittent flow, International Journal of Heat and Fluid Flow, 2001,Vol. 22, No. 5, pp. 543–551.

[6]   Hernandez-Perez, V. Gas-liquid two-phase flow in inclined pipes. PhD thesis, University of Nottingham (2008).

[7]   STAR-CD Version 4.10 and STAR-CCM+ Documentation, 2009 CD-adapco.

[8]   Erdal, F. M., Shirazi, S. A., Shoham, O., Kouba, G. E. (1997), CFD Simulation of Single-Phase and Two-Phase Flow in Gas-Liquid Cylindrical Cyclone Separators, Society of Petroleum Engineers 36645.

[9]   Van Baten, J. M. and Krishna, R., Eulerian simulations for determination of the axial dispersion of liquid and gas phases in bubble columns operating in the churn-turbulent regime, Chemical Engineering Science 56 (2001) 503–512.

[10]   Jeong, H. M., Lee, Y. H., Ji, M. K., Bae, K. Y., and Chung, H. S., Natural convection heat transfer estimation from a longitudinally finned vertical pipe using CFD, Journal of Mechanical Science and Technology 23 (2009) 1517~1527, DOI: 10.1007/s12206-009-0406-4.

[11]   Ma, L., Ingham, D. B. and Wen, X., 1998, A finite volume method for fluid flow in polar cylindrical grids, International Journal for Numerical Methods in Fluids, Volume 28 Issue 4, Pages 663–677.

[12]   Azzopardi B.J., Hernandez Perez, V., Kaji R., Da Silva M.J., Beyer M., and Hampel U., (2008), Wire mesh sensor studies in a vertical pipe, HEAT 2008, Fifth International Conference on Transport Phenomena in Multiphase Systems, Bialystok, Poland.

[13]   Hernandez-Perez, V., Abdulkareem, L. and Azzopardi, B.J., Effects of physical properties on the behaviour of Taylor bubbles, WIT Fifth International Conference on Computational Methods in Multiphase flow 2009. New Forest UK. 15–17 June 2009, p. 355.

[14]   Da Silva, M.J., Schleicher E. & Hampel, U., Capacitance wire-mesh sensor for fast measurement of phase fraction distributions. Meas. Sci. Tech. Vol. 18, pp. 2245–2251, 2007.

[15]   Hirt, C. W. and Nichols, B. D., Volume of Fluid (VOF) Method for the Dynamics of Free Boundaries, J. Comp. Phys., 1981, Vol. 39, pp. 201.

[16]   Ubbink, O. 1997, Numerical prediction of two fluid systems with sharp interfaces, PhD thesis, University of London.

[17]   Muzaferija, S., Peric, M., Computation of free surface flows using interface-tracking and interface-capturing methods, Chap. 2 in O. Mahrenholtz and M. Markiewicz (eds.), Nonlinear Water Wave Interaction, Computational Mechanics Publication, WIT Press, Southampton, 1999.

[18]   Brackbill, J.U., Kothe, D.B., and Zemach, C. 1992. A continuum method for modeling surface tension, J. Comput. Phys., 100, pp. 335–354.

[19]   Launder, B. and Spalding, D., The numerical computation of turbulent flows, Computer Methods in Applied Mechanics and Engineering, 1974, Vol. 3, pp. 269–289.

[20]   Shen, Y.M. , Ng, C.O. and Zheng, Y.H., Simulation of wave propagation over a submerged bar using the VOF method with a two-equation k–epsilon turbulence modeling, Ocean Eng. 31 (2004), pp. 87–95.

[21]   Versteeg, H.K. and Malalasekera, W., 2007. An Introduction to Computational Fluid Dynamics: the Finite Volume Method. 2nd ed. Pearson Educational Limited.

[22]   Patankar, S.V., Spalding, D.B. (1972), "A calculation procedure for heat, mass and momentum transfer in three dimensional parabolic flows", Int. J. of Heat and Mass Transfer, Vol. 15 pp.1787.

[23]   Pinto, A. M. F. R. and Campos, J. B. L. M., Coalescence of two gas slugs rising in a vertical column of liquid, Chemical Engineering Science, 1996, Vol. 51, No. 45–54.

[24]   Pinto, A. M. F. R., Coelho Pinheiro, M. N., and Campos, J. B. L. M., Coalescence of two gas slugs rising in a co-current flowing liquid in vertical tubes, Chemical Engineering Science, 1998, Vol. 53, pp. 2973–2983.

[25]   Shemer, L., Gulitski, A., and Barnea, D., Velocity field in the Taylor bubble wake measurements in pipes of various diameters, 24nd European Two-phase Flow Group Meeting, Geneva, 2004.

[26]   Szalinski, L.A. Abdulkareem, M.J. Da Silva, S. Thiele, M. Beyer, D. Lucas, V. Hernandez Perez, B.J. Azzopardi, U. Hampel, Comparative study of gas-oil and gas-water two-phase flow in a vertical pipe, Chemical engineering science. 65, Issue 12, 3836–3848.